Published for SISSA by Springer

Received: June 25, 2013
Revised: September 18, 2013
Accepted: October 28, 2013
Published: November 11, 2013

JHEP11(2013)082

Gluon saturation scale from the KGBJS equation

Krzysztof Kutak and Dawid Toton

Instytut Fizyki Jądrowej im. H. Niewodniczańskiego, Radzikowskiego 152, 31-342 Kraków, Poland

E-mail: krzysztof.kutak@ifj.edu.pl, dawid.toton@ifj.edu.pl

Abstract: The CCFM equation and its extended form with a quadratic term (KGBJS equation) are solved with fixed and running coupling constant. The solution of the KGBJS equation is compared to gluon densities resulting from the CCFM and BK equations. As the saturation scale Q_s now becomes available as a function of the hard scale p we observe that low values of p impede its growth with $\frac{1}{x}$. Also, at values much larger than partons transversal momentum the saturation effects become independent on the hard scale what we call liberation of saturation scale. We also introduce the hard-scale-related saturation scale P_s and investigate its energy dependence. We observe that the new scale as a function of x decreases starting from the value of transversal momentum of gluon.

Keywords: QCD Phenomenology, Phenomenological Models

ArXiv ePrint: 1306.3369

doi:10.1007/JHEP11(2013)082

Contents

JHEP11(2013)082

1 Introduction

We consider hadronic scattering in the limit of high center-of-mass energy, where the energy is the largest scale in the problem. Perturbative treatment of processes with high momentum transfer at high energies leads to decomposition of the cross section into hard matrix element and gluon density [1, 2] which is a function of the longitudinal momentum fraction x and transverse momentum $\mathbf{k}$ of a gluon as well as a scale p related to a hard process. The gluon density obtained in such a setup at not too large parton densities obeys the CCFM [3–5] equation. The equation sums up gluons with a condition of strong ordering in angle and can be viewed as a bridge between BFKL and DGLAP regimes. The particularly interesting is however to apply the CCFM framework to saturation physics [1] in order to investigate saturation with the help of exclusive processes like for example di-jet production at the LHC [6–10]. The first step towards introducing saturation in the CCFM framework has been done in [11–13] applying the absorptive boundary method [14] in order to suppress gluon density at low values of gluon's transversal momentum $\mathbf{k}$. Another approach has been developed in [15–17] where the extension of CCFM to allow for dynamical gluon saturation has been proposed. The proposed equations (for Weizsäcker-Williams gluon density (KGBJS) in [15, 16] and unintegrated gluon density in [17]) have structure similar to the resummed BK equation [15] since the form factors in the new equations (Sudakov and non-Sudakov) are linked by the limit procedure to the Regge form factor being present in the resummed BK equation.

In this paper we solve KGBJS and the CCFM equations with running and fixed coupling constants. In order to quantify effects of coherence, running couplig effects and hard scale dependence we take into account only hard emissions [13, 18–23] and compare the solution to solution of the BK equation which is hard scale independent and where the running coupling effects are well understood. Working with this approximation we can make easier comparison of our results for saturation scale with those obtained in [23].

We also study in detail the nonlinear effects by calculating the emergent saturation scale in the KGBJS equation. The novel feature of the saturation scale is its nontrivial dependence on the hard scale related variable p. We observe that when the hard scale related variable is much larger than the $\mathbf{k}$ of gluon the saturation scale stops to depend on it and the BK limit is reached. We call this effect liberation of saturation scale due to relaxing of phase space constraint. The paper is organized as follows. In the section two we present solutions of the KGBJS and CCFM equations in case of fixed and running coupling constants and study the effect of running coupling on the solutions. In section three we study the saturation effects in the KGBJS equation by analyzing the properties of the saturation scale as emerged due to nonlinearities. We compare that scale to the one generated via the BK evolution [24, 25]. As the equation depends on a hard scale we also introduce hard scale related saturation scale P_s.

2 The CCFM evolution equation and its nonlinear extension

2.1 Hard emissions approximation and running coupling effects

The KGBJS equation reads:[1]

$$\mathcal{E}(x,k^2,p) = \mathcal{E}_0(x,k^2,p) + \int \frac{d^2\bar{\mathbf{q}}}{\pi\bar{q}^2}\int_{x/x_0}^{1-Q_0/\bar{q}} dz\,\theta(p-z\bar{q})P_{gg}(z,k,\bar{q},p)\Bigg[\mathcal{E}\left(\frac{x}{z},k'^2,\bar{q}\right) - \frac{1}{\pi R^2}\bar{q}^2\delta(\bar{q}^2-k^2)\,\mathcal{E}^2\left(\frac{x}{z},\bar{q}^2,\bar{q}\right)\Bigg] \tag{2.1}$$

where

$$P_{gg}(z,k,\bar{q},p) = \bar{\alpha}_s\Delta_s(p,z\bar{q})\left(\frac{\Delta_{ns}(z,k,\bar{q})}{z}+\frac{1}{1-z}\right). \tag{2.2}$$

The momentum vector associated with i-th emitted gluon is

$$q_i = \alpha_i\, p_P + \beta_i\, p_e + q_{t\,i}. \tag{2.3}$$

The variable p in (2.1) is defined via $\bar{\xi} = p^2/(x^2 s)$ where $\frac{1}{2}\ln(\bar{\xi})$ is a maximal rapidity which is determined by the kinematics of hard scattering, $\sqrt{s}$ is the total energy of the collision and $k' = |\boldsymbol{k} + (1-z)\bar{\boldsymbol{q}}|$, $\bar{\alpha} = N_c\alpha_s/\pi$. We also define $k \equiv |\mathbf{k}|$. The momentum $\bar{\mathbf{q}}$ is the transverse rescaled momentum of the emitted gluon, and is related to $\mathbf{q}$ by $\bar{\mathbf{q}} = \mathbf{q}/(1-z)$ and $\bar{q} \equiv |\bar{\mathbf{q}}|$, and Q_0 is a cutoff on gluons momentum.
The form factor Δ_s accompanies the $1-z$ pole and it reads:

$$\Delta_s(p,z\bar{q}) = \exp\left(-\bar{\alpha}_s\ln\frac{p}{z\bar{q}}\ln\frac{z\bar{q}p}{Q_0^2}\right) \tag{2.4}$$

[1] In the nonlinear term we did not include the $1/(1-z)^2$ as it has been suggested in [28]. In the present paper we are going to solve the equation in the approximate form where the eventual problem observed in [28] does not show up. We are going to address the problem of proposed modification of the solution of the full equation in the future.

JHEP11(2013)082

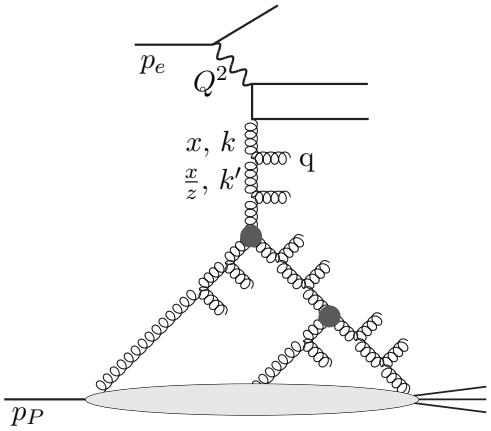

Figure 1. Schematic illustration of kinematical variables used in the eq. (2.1).

while the form factor Δ_{ns} accompanying the $1/z$ pole accounts for angular ordering. We use its form as proposed in [19]:

$$\Delta_{ns}(z,k,q) = \exp\left(-\bar{\alpha}_s \ln\frac{z_0}{z}\ln\frac{k^2}{z_0 z q^2}\right) \tag{2.5}$$

where $z_0 = \frac{k}{q}$ for $z < \frac{k}{q} < 1$ and outside the interval it assumes the bounding values, $z_0 = z$ when $\frac{k}{q} < z$ and $z_0 = 1$ when $\frac{k}{q} > 1$. The more inclusive form of the equation follows if we set the Sudakov form-factor Δ_s to unity and neglect the contribution from the soft emissions i.e. $\frac{1}{1-z}$ pole in P_{gg} (and no z cutoff). We obtain:

$$\begin{aligned}\mathcal{E}(x,k,p) = \mathcal{E}_0(x,k,p) + \int_x^{x_0}\frac{\mathrm{d}w}{w}\int_0^{\infty}\frac{\mathrm{d}q^2}{q^2}\int_0^{\pi}\frac{\mathrm{d}\phi}{\pi}\theta\left(p - zq\right)P_{gg}(z,k,q)\mathcal{E}\left(w,k',q\right)\\ -\frac{1}{\pi R^2}\int_x^{x_0}\frac{\mathrm{d}w}{w}\theta(p-zk)P_{gg}(z,k,k)\mathcal{E}^2\left(w,k,k\right)\end{aligned} \tag{2.6}$$

where $z = \frac{x}{w}$ under both of the $\mathrm{d}w$ integrals (from now on when we will use the KG-BJS acronym we will refer to equation (2.6)). The splitting function, with running α_s following [19], is simplified to:

$$P_{gg}(z,k,q) = \bar{\alpha}_s(k^2)\frac{\Delta_{ns}(z,k,q)}{z}. \tag{2.7}$$

The parameter characterizing the target is chosen to be $R = 10/\sqrt{\pi}$ and the starting point of evolution is chosen to be $x_0 = 10^{-2}$. For the future phenomenological applications we investigate the effect of running coupling constant on the solution of considered equation.

JHEP11(2013)082

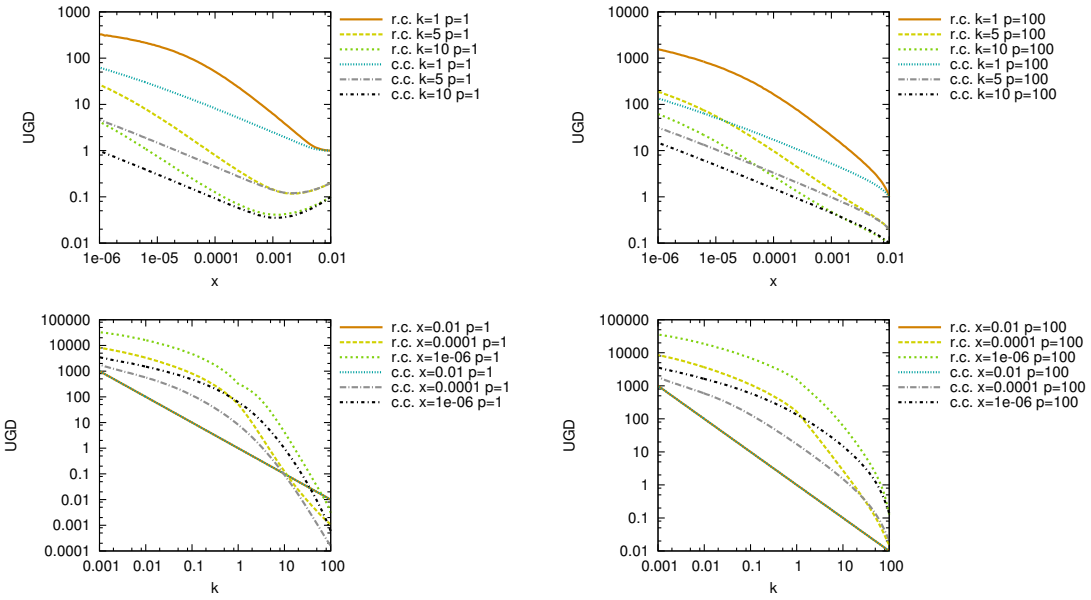

Figure 2. Comparison of solutions of the KGBJS equation with constant ($\bar{\alpha}_s = 0.2$) and running coupling (eq. (2.8)).

The running coupling corrections were included in the following manner:[2]

$$\alpha_s(k^2) = \frac{12\pi}{33 - 2n_f} \frac{1}{\ln \frac{\max\{k^2, k^2_{freeze}\}}{\Lambda^2_{QCD}}} \tag{2.8}$$

with $n_f = 3$, $\Lambda_{QCD} = 0.2$ GeV and the $\max\{\cdot\}$ notation makes k bounded by $k_{freeze} = 1$ GeV. The initial condition we choose to be:

$$\mathcal{E}_0(x, k, p) = \frac{\text{GeV}}{k} \mathrm{e}^{-\bar{\alpha}_s(k^2) \ln \frac{x_0}{x} \ln \frac{k^2}{\mu^2}}. \tag{2.9}$$

The extra x-dependent term follows from the resummation procedure for the BK equation [15], and is necessary in order for the equation in a new form to match the solution in the original form [26]. The extra parameter μ is a small cut-off momemtum introduced by the procedure of resummation. We use this extra factor also for the KGBJS equation in order to study differences in the evolution between these two equations.

A two solutions of the KGBJS equation are presented on figure 2. First of the plots, shows the x dependence of the solutions at small $p = 1$ GeV. The considered form of the initial condition makes the distributions fall and attain a minimum (visible just above $x = 0.001$), whereas solution obtained with simplified $\mathcal{E}_0$ (figure 3) and solution of the BK equation, as depicted on figure 7, don't suffer this. The minimum suggests that the KGBJS

[2] In the future we are going to implement the running coupling constant as obtained in [27]. For our present study this is however not crucial since our main point is the behavior of the saturation scale as a function of a hard scale and this should not change dramatically with another prescription for running of the coupling constant.

JHEP11(2013)082

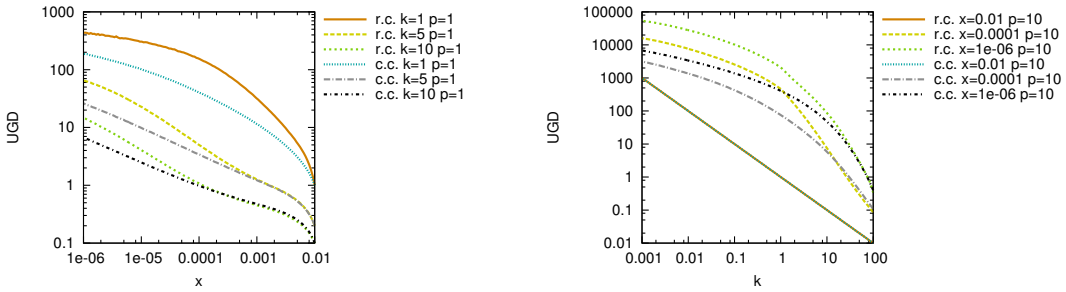

Figure 3. Comparison of solutions of the KGBJS equation with constant and running coupling; the initial condition $\mathcal{E}_0(x,k,p) = \frac{\mathrm{GeV}}{k}$ with no Regge factor is taken; the calculations are otherwise identical as for figure 2.

does not grow as fast with decreasing x as BK and that the form of initial condition given by (2.9) is not optimal for KGBJS and CCFM (at $x = 10^{-2}$ the solutions are equivalent) and that more sophisticated initial condition has to be provided. For example in [20] the initial condition included the non-Sudakov form factor and angular ordering and as we see from plots on figure 4 in [20] the solution of CCFM does not have a minimum along x. The solutions shown on figure 3 also grow monotonically, but with simple initial condition that is flat along x. We see also on figure 2 that the effect of running coupling constant as compared to the fixed value at $\alpha_s = 0.2$ leads to faster growth of the density and is more pronounced when the hard scale is larger. This can be observed for no too large k, so that $\alpha_s(k^2) > 0.2$. On the other hand for high enough k we can expect that small values of $\alpha_s(k^2)$ cause an opposite effect and the solution obtained with constant α_s grows faster. Figure 4, (left) shows a solution of the BK equation with range of the transverse momentum large enough to cover both the cases (and with $R = 1/\pi$ to make the discussed effect more visible). With decreasing x the saturation scale Q_s rises. As it enters the region where $\alpha_s(Q_s^2) < 0.2$, the solution obtained with constant $\alpha_s = 0.2$ grows faster. This prompts the saturation to come sooner, for given transverse momentum, as compared to the case with running coupling. We can thus understand why Q_s generated by the BK equation is observed to grow faster when α_s is set to 0.2 as compared to its value given by eq. (2.8) (see also coordinate space analysis done in [30]). Solutions of KGBJS have a similar property for the highest values of p (figure 4, (right). Running of the coupling attenuates growth of the gluon density for high k and for lower vlues of k the effect is opposite. If the scale p is lower, the relation is less clear. Namely, the solution with running α_s on figure 2 at $p = 1$ GeV and around $k = 50$ GeV dominates over the constant α_s solution and the difference grows bigger with higher k. This is due to small values of $\alpha_s(k^2)$ entering the exponent in the Regge factor included in the initial condition. Indeed, if this factor is omitted, the r.c. solutions falls below the c.c. solution (figure 3, right).

The particularly interesting is the behavior of CCFM and KGBJS as a function of hard scale related variable p. The figure 6 shows that the solution of the equations is a constant function of the p variable as it is larger than transversal momentum of gluon. This effect can be understood by investigating the $\theta(p - z\,q)$ function in the considered equations. If

JHEP11(2013)082

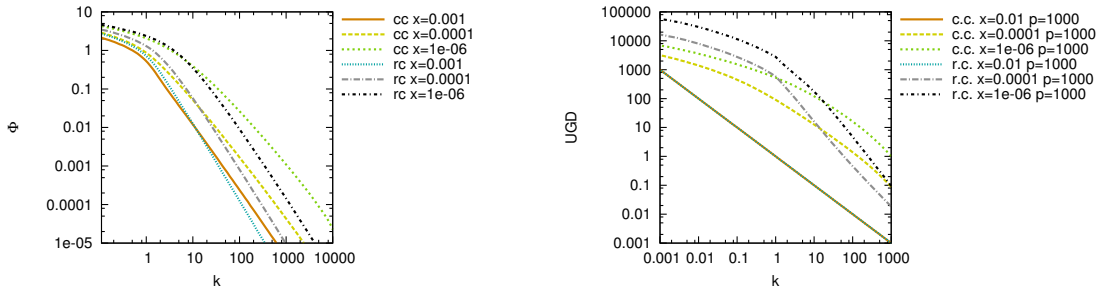

Figure 4. Comparison of solutions of evolution equations with constant ($\bar{\alpha}_s = 0.2$) and running coupling (eq. (2.8)). Left: BK equation with Gaussian initial condition; right: KGBJS, plots for high p.

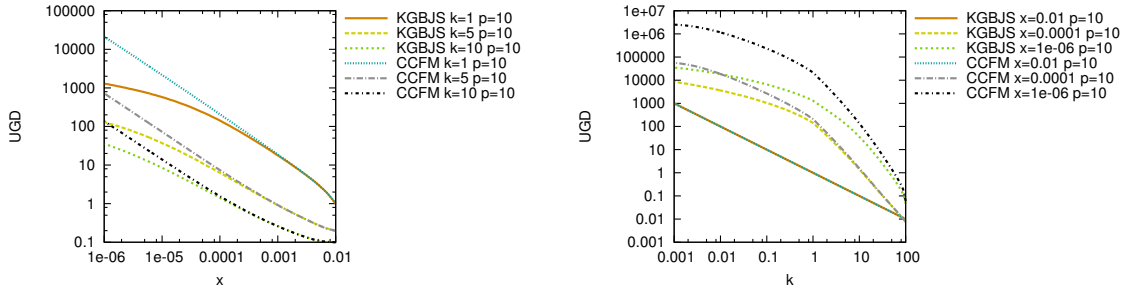

Figure 5. Comparison of solutions of the KGBJS and CCFM equations (running $\bar{\alpha}_s$).

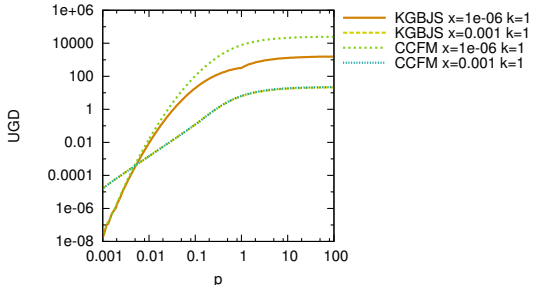

Figure 6. Hard scale dependence of the CCFM and KGBJS equations.

the variable p is larger than q than the theta function sets to one and the angular ordering is relaxed. We expect this will have interesting implications for the saturation scale generated by the KGBJS equation. The plots on figure 5 compare solutions of CCFM and KGBJS. We see the damping of the gluon density due to nonlinearity in case of KGBJS equation as we go towards low x and low k values.

JHEP11(2013)082

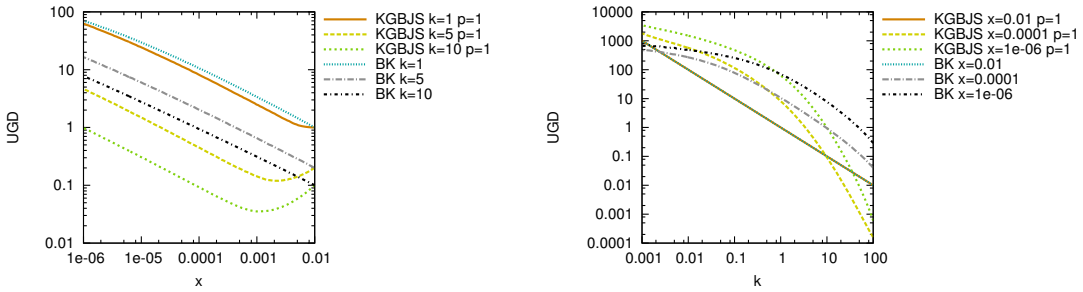

Figure 7. Comparison of solutions of the KGBJS and BK equations (constant $\bar{\alpha}_s$).

2.2 KGBJS and BK equations – comparison

The Balitsky-Kovchegov equation in the resummed form reads:

$$\Phi(x,k^2) = \tilde{\Phi}^0(x,k^2) + \overline{\alpha}_s \int_{\frac{x}{x_0}}^1 d\,z \int \frac{d^2\mathbf{q}}{\pi q^2}\,\theta(q^2-\mu^2)\frac{\Delta_R(z,k,\mu)}{z}\left[\Phi\left(\frac{x}{z},|\mathbf{k}+\mathbf{q}|^2\right)\right.$$
$$\left. - \frac{1}{\pi R^2} q^2\delta(q^2-k^2)\,\Phi^2\left(\frac{x}{z},q^2\right)\right]. \tag{2.10}$$

The Regge form factor assumes the form:

$$\Delta_R = e^{-\bar{\alpha}_s \ln 1/z \ln k^2/\mu^2} \tag{2.11}$$

where μ is the resolution parameter. We assumed $\mu = 0.01$ GeV in the calculations. The equation above has been solved in [26] and its solution has been shown to be the same as the unresummed BK equation. It is instructive to compare the numerical solutions of the two equations in order to quantify the role of the angular ordering and dependence on the hard scale of the gluon density. In figure 7 we compare solutions of the KGBJS and the BK equations for fixed values of the coupling constant. We see that as expected the slope of the solution of KGBJS equation (see figure 2, right) is steeper due to suppression by the non-Sudakov form factor of large k values. We also see that at low k the saturation is weaker in the KGBJS equation as compared to BK. This could be understood by inspecting the nonlinear term of (2.6). We see that the $\bar{q}$ integral in eq. (2.1) applied to the nonlinear part makes the non-Sudakov form factor to become:

$$\Delta_{ns}(z,k,k) = e^{-\bar{\alpha}_s \ln^2 1/z}. \tag{2.12}$$

This is to be compared with the Regge form factor in eq. (2.11). We see that for the fixed value of k the nonlinear term in the KGBJS equation is more suppressed as compared to the BK equation therefore it leads to weaker saturation.

3 Saturation of the exclusive gluon distribution

To shed light on the importance of nonlinear corrections in the KGBJS, we consider contour lines of the relative difference between solutions:

$$\beta(x,k,p) = \frac{|\mathcal{E}_{CCFM}(x,k,p) - \mathcal{E}_{KGBJS}(x,k,p)|}{\mathcal{E}_{CCFM}(x,k,p)}. \tag{3.1}$$

JHEP11(2013)082

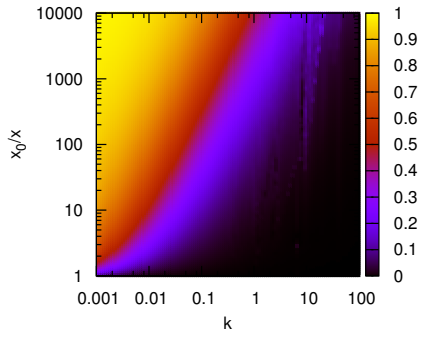

Figure 8. Relative difference β between solutions of BK and BFKL.

The traditional saturation scale Q_s, i.e. transversal momentum for which the effects of nonlinearity are noticeable, we define as:

$$\beta(x, Q_s(x,p), p) = const. \tag{3.2}$$

Such quantity has been already defined for the BK equation [29]:

$$\beta(x, Q_s(x)) = const \tag{3.3}$$

with

$$\beta(x,k) = \frac{|\Phi_{BFKL}(x,k) - \Phi_{BK}(x,k)|}{\Phi_{BFKL}(x,k)} \tag{3.4}$$

where $\Phi_{BK}(x,k^2)$ is a solution of (2.10).

The quantity defined above, as observed in [29], has somewhat different slope compared to the saturation scale defined as a scale where the dipole amplitude is $1/2$. However, as we see from the plots it is a good measure of the strength of nonlinearities. The plot of β on figure 8 confirms the familiar growth of the saturation scale, which can be seen as $1/x$ is increasing upwards on the plot.

The most interesting and novel effect as compared to the BK equation is the dependence of the saturation scale on the hard scale related variable p. Several cross-sections of the β function (in the presentation we limit ourselves to the running coupling case and the form of initial condition with the Regge form factor since the effect we observe is universal) on figures 9, 10 indicate regions where KGBJS solutions diverge from results of the linear evolution. The $k > p$ areas of the plots show that the nonlinear effects enter when the x_0/x is rather small. We also see that at $p \approx k$ the saturation line changes slope to larger value and as we go towards larger k the saturation is weaker. However with growing p the nonlinear effects become larger the slope becomes approximately constant and gluons get blocked by saturation. This is the consequence of larger available phase space (note the $\theta(p - z\bar{q})$ factor in the kernel of the eq. (2.1)) for larger p which allows for the gluon density to grow and therefore to come at values where the nonlinear effects start to be important. Eventually in phase space region where $p \gg k$ the KGBJS equation becomes

JHEP11(2013)082

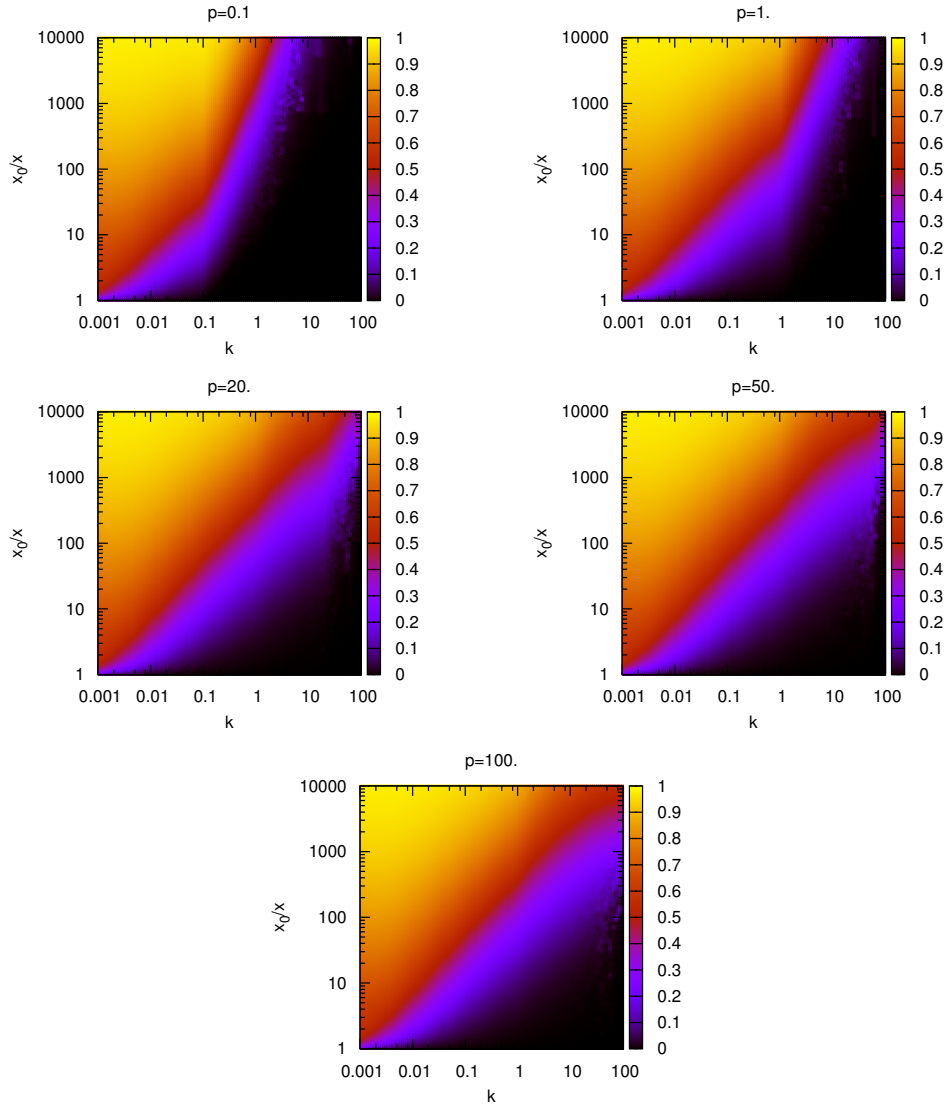

Figure 9. The β function (cross-sections for constant p). Solutions with running α_s.

independent on the hard scale and therefore the saturation scale stops to depend on it and gets liberated. In this limit the maximal value of it is given and BK regime is reached. Similar effect has been already observed in [23] with application of the absorptive boundary method (see for example figure 20 of [23], adjust it to have Y axis vertical and compare it to presented here figure 10). The difference is however in the strength of the effect since in the absorptive boundary method the authors of [23] set arbitrarily the value of gluon density below the saturation scale to a constant value while in our approach we allow for dynamical evolution and growth of gluon density. The effect, called here liberation of saturation scale, is linked to the so-called saturation of saturation scale expected in [15, 23]. Since as we go towards the smaller values of p we see that the saturation bends towards the x_0/x axis and its growth is hindered. Another aspect of the equation (2.6) is that it

JHEP11(2013)082

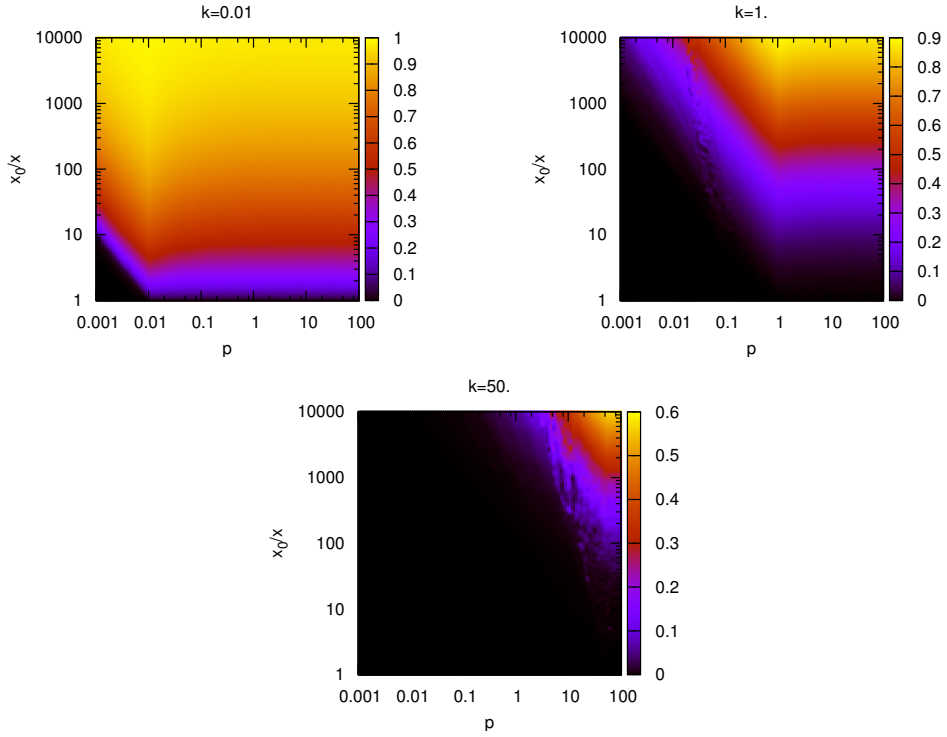

Figure 10. The β function (cross-sections for constant k). Solutions with running α_s.

allows to define p-related saturation scale P_s as:

$$\beta\left(x, k, P_s(x,k)\right) = \text{const}\,. \tag{3.5}$$

For fixed k, this function becomes a line, $P_s(x)$. It indicates how the hard scale required to enter the saturation regime changes with x. On figure 10 we plot the relative difference as defined in eq. (3.5) as a function of p for varying k. First of all we notice nontrivial relation between the values of k and p and nonlinearities. If the value of p is smaller than k there is not much phase space available for growth of the gluon and the smaller p is the lower x has to be in order for the nonlinear effects to be visible. For values of $p > k$ the slope of the saturation region is roughly zero and for all values of p the saturation enters at the same values of x. We can say that the hard scale required to unveil the saturation abruptly descends from infinity for some k-dependent x.

4 Conclusions

In this paper we performed numerical study of the simplified form of the KGBJS and CCFM evolution equations with running and fixed coupling constant. We compared the obtained solutions to the solution of the BK equation to investigate the interplay of saturation and coherence. We investigated the role of nonlinearity in the KGBJS equation by studying the emergent saturation scale i.e. the relative differences between solutions of the KGBJS and CCFM equations. Due to the dependence of the KGBJS equation on the hard scale the saturation scale has been shown to depend on it in a nontrivial way. In particular,

JHEP11(2013)082

when the hard scale gets much larger than the k of the gluon, the saturation scale stops to depend on hard scale value and liberates itself and is independent function of hard scale. Finally we introduced hard scale related saturation scale P_s i.e. measure of importance of nonlinearity as a function of hard scale and energy for fixed values of k. The analysis of the new scale shows that if the region when the k of the gluon is larger than the hard scale the phase space is limited and the gluon density in order to be sensitive to nonlinear effects has to be evaluated at quite low x. On the contrary if the scale p is larger than gluon transversal momentum k the x values when the nonlinearities are important become quite large. The presented analysis of the KGBJS equation is going to be extended in the future. In particular, the impact on saturation of the Sudakov form factor and full splitting function is going to be investigated as well as the properties of solution of equation written directly for the unintegrated gluon density in [17].

Acknowledgments

We would like to thank K. Bozek, M. Deak, K. Golec-Biernat, H. Jung, R. Peschanski, W. Placzek, K. Slawinska for useful discussions.

Krzysztof Kutak and Dawid Toton were supported during this research by Narodowe Centrum Badań i rozwoju with grant LIDER/02/35/L-2/10/NCBiR/2011.

References

[1] L. Gribov, E. Levin and M. Ryskin, *Semihard Processes in QCD*, *Phys. Rept.* **100** (1983) 1 [INSPIRE].

[2] S. Catani, M. Ciafaloni and F. Hautmann, *High-energy factorization and small x heavy flavor production*, *Nucl. Phys.* **B 366** (1991) 135 [INSPIRE].

[3] M. Ciafaloni, *Coherence Effects in Initial Jets at Small Q^2/s*, *Nucl. Phys.* **B 296** (1988) 49 [INSPIRE].

[4] S. Catani, F. Fiorani and G. Marchesini, *Small x Behavior of Initial State Radiation in Perturbative QCD*, *Nucl. Phys.* **B 336** (1990) 18 [INSPIRE].

[5] S. Catani, F. Fiorani and G. Marchesini, *QCD Coherence in Initial State Radiation*, *Phys. Lett.* **B 234** (1990) 339 [INSPIRE].

[6] M. Deak, F. Hautmann, H. Jung and K. Kutak, *Forward Jet Production at the Large Hadron Collider*, *JHEP* **09** (2009) 121 [arXiv:0908.0538] [INSPIRE].

[7] M. Deak, F. Hautmann, H. Jung and K. Kutak, *Jets in the forward region at the LHC*, arXiv:0908.1870 [INSPIRE].

[8] M. Deak, F. Hautmann, H. Jung and K. Kutak, *Forward-Central Jet Correlations at the Large Hadron Collider*, arXiv:1012.6037 [INSPIRE].

JHEP11(2013)082

[9] K. Kutak and S. Sapeta, *Gluon saturation in dijet production in p-Pb collisions at Large Hadron Collider*, *Phys. Rev.* **D 86** (2012) 094043 [arXiv:1205.5035] [INSPIRE].

[10] CMS collaboration, *Measurement of the inclusive production cross sections for forward jets and for dijet events with one forward and one central jet in pp collisions at* $\sqrt{s} = 7$ *TeV*, *JHEP* **06** (2012) 036 [arXiv:1202.0704] [INSPIRE].

[11] K. Kutak and H. Jung, *Saturation effects in final states due to CCFM with absorptive boundary*, *Acta Phys. Polon.* **B 40** (2009) 2063 [arXiv:0812.4082] [INSPIRE].

[12] E. Avsar and E. Iancu, *BFKL and CCFM evolutions with saturation boundary*, *Phys. Lett.* **B 673** (2009) 24 [arXiv:0901.2873] [INSPIRE].

[13] E. Avsar and E. Iancu, *CCFM Evolution with Unitarity Corrections*, *Nucl. Phys.* **A 829** (2009) 31 [arXiv:0906.2683] [INSPIRE].

[14] A. Mueller and D. Triantafyllopoulos, *The energy dependence of the saturation momentum*, *Nucl. Phys.* **B 640** (2002) 331 [hep-ph/0205167] [INSPIRE].

[15] K. Kutak, K. Golec-Biernat, S. Jadach and M. Skrzypek, *Nonlinear equation for coherent gluon emission*, *JHEP* **02** (2012) 117 [arXiv:1111.6928] [INSPIRE].

[16] K. Kutak, *Nonlinear extension of the CCFM equation*, arXiv:1206.1223 [INSPIRE].

[17] K. Kutak, *Resummation in nonlinear equation for high energy factorisable gluon density and its extension to include coherence*, *JHEP* **12** (2012) 033 [arXiv:1206.5757] [INSPIRE].

[18] G. Marchesini, *QCD coherence in the structure function and associated distributions at small x*, *Nucl. Phys.* **B 445** (1995) 49 [hep-ph/9412327] [INSPIRE].

[19] J. Kwiecinski, A.D. Martin and P. Sutton, *The gluon distribution at small x obtained from a unified evolution equation*, *Phys. Rev.* **D 52** (1995) 1445 [hep-ph/9503266] [INSPIRE].

[20] J. Kwiecinski, A.D. Martin and P. Sutton, *The description of F2 at small x incorporating angular ordering*, *Phys. Rev.* **D 53** (1996) 6094 [hep-ph/9511263] [INSPIRE].

[21] G. Bottazzi, G. Marchesini, G. Salam and M. Scorletti, *Structure functions and angular ordering at small x*, *Nucl. Phys.* **B 505** (1997) 366 [hep-ph/9702418] [INSPIRE].

[22] G. Bottazzi, G. Marchesini, G. Salam and M. Scorletti, *Small x one particle inclusive quantities in the CCFM approach*, *JHEP* **12** (1998) 011 [hep-ph/9810546] [INSPIRE].

[23] E. Avsar and A.M. Stasto, *Non-linear evolution in CCFM: The interplay between coherence and saturation*, *JHEP* **06** (2010) 112 [arXiv:1005.5153] [INSPIRE].

[24] I. Balitsky, *Operator expansion for high-energy scattering*, *Nucl. Phys.* **B 463** (1996) 99 [hep-ph/9509348] [INSPIRE].

[25] Y.V. Kovchegov, *Small-x F2 structure function of a nucleus including multiple Pomeron exchanges*, *Phys. Rev.* **D 60** (1999) 034008 [hep-ph/9901281] [INSPIRE].

[26] K. Kutak, W. Płaczek and D. Toton, *Numerical solution of the integral form of the resummed Balitsky-Kovchegov equation*, *Acta Phys. Polon.* **B 44** (2013) 1527 [arXiv:1303.0431] [INSPIRE].

[27] Y.V. Kovchegov and H. Weigert, *Quark loop contribution to BFKL evolution: Running coupling and leading-N(f) NLO intercept*, *Nucl. Phys.* **A 789** (2007) 260 [hep-ph/0612071] [INSPIRE].

JHEP11(2013)082

[28] M. Deak, *Estimation of saturation and coherence effects in the KGBJS equation — a non-linear CCFM equation*, arXiv:1209.6092 [INSPIRE].

[29] K. Kutak and A. Stasto, *Unintegrated gluon distribution from modified BK equation*, *Eur. Phys. J.* **C 41** (2005) 343 [hep-ph/0408117] [INSPIRE].

[30] J. Albacete, N. Armesto, J. Milhano, C. Salgado and U. Wiedemann, *Numerical analysis of the Balitsky-Kovchegov equation with running coupling: Dependence of the saturation scale on nuclear size and rapidity*, *Phys. Rev.* **D 71** (2005) 014003 [hep-ph/0408216] [INSPIRE].

JHEP11(2013)082